Supporting Information

Designing Few-Layered Graphitic Carbons with Atomic-sized Cobalt Hydroxide by Harnessing Hollow Metal-Organic Frameworks

Eun Jin Cho,[a‡] Bo-Min Kim,[a‡] WooYeon Moon,[b] Dong Gyu Park,[c] Young-Wan Ju,[d] Won Ho Choi*[e] and Jeeyoung Shin*[a,c]

[a] *Department of Mechanical Systems Engineering, Sookmyung Women's University, Seoul 04310, Republic of Korea*

[b] *Department of Chemical and Biological Engineering, Sookmyung Women's University, Seoul 04310, Republic of Korea*

[c] *Institute of Advanced Materials and Systems, Sookmyung Women's University, Seoul, 04310, Republic of Korea*

[d] *Department of Chemical Engineering, College of Engineering, Wonkwang University, Iksan-si 54538, Republic of Korea*

[e] *Department of Petrochemical Materials, Chonnam National University, Yeosu-si 59631, Republic of Korea*

‡These authors equally contributed to this manuscript.

**E-mail: wonhochoi@jnu.ac.kr, jshin@sookmyung.ac.kr*

Figure S34. Galvanostatic charge-discharge curve of c-ZIF-67 at 1 to 10 $A \cdot g^{-1}$

Table S1. BET Specific surface area, average pore diameter, and total pore volume of ZIF-67, c-ZIF-67, hZIF-8, and c-hZIF-8

Table S2. The specific capacitance of $Co(OH)_2 \subset$c-hZIF-8 at different current densities

Table S3. The specific capacitance of $Co(OH)_2 \subset$c-ZIF-67 at different current densities

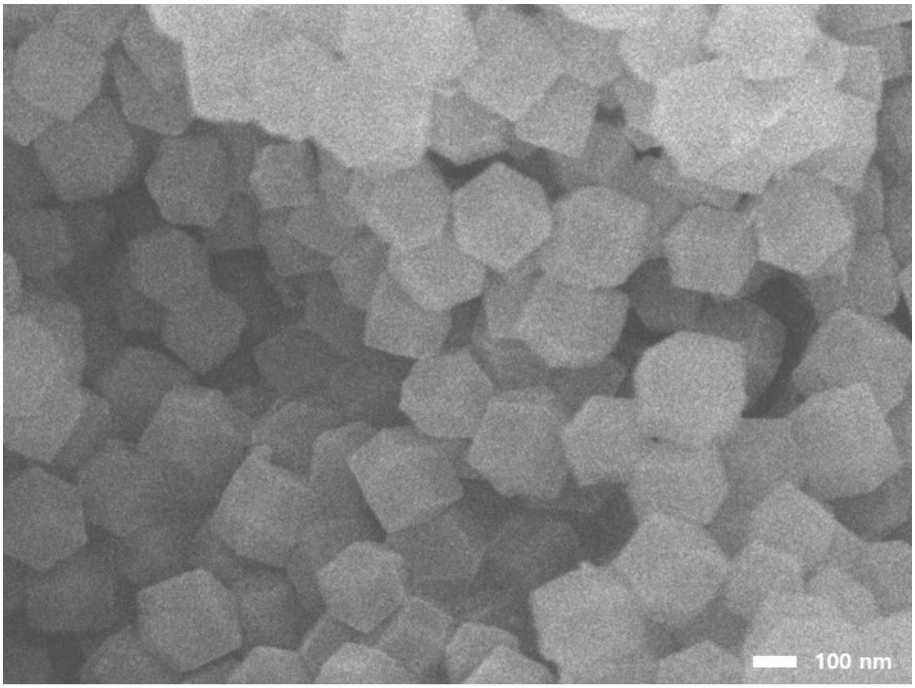

Figure S1. SEM image of ZIF-67

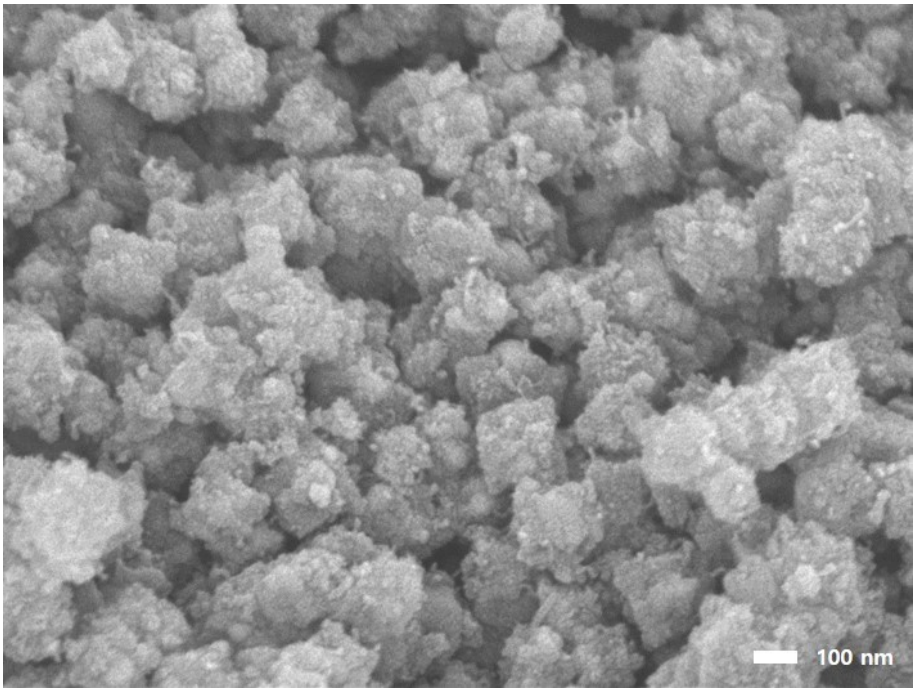

Figure S2. SEM image of c-ZIF-67

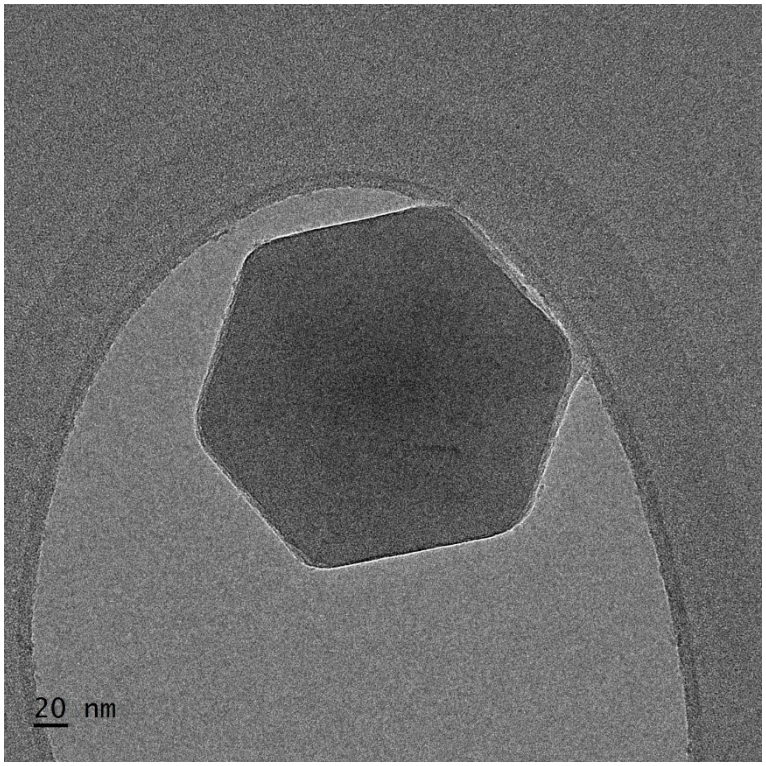

Figure S3. TEM image of ZIF-67

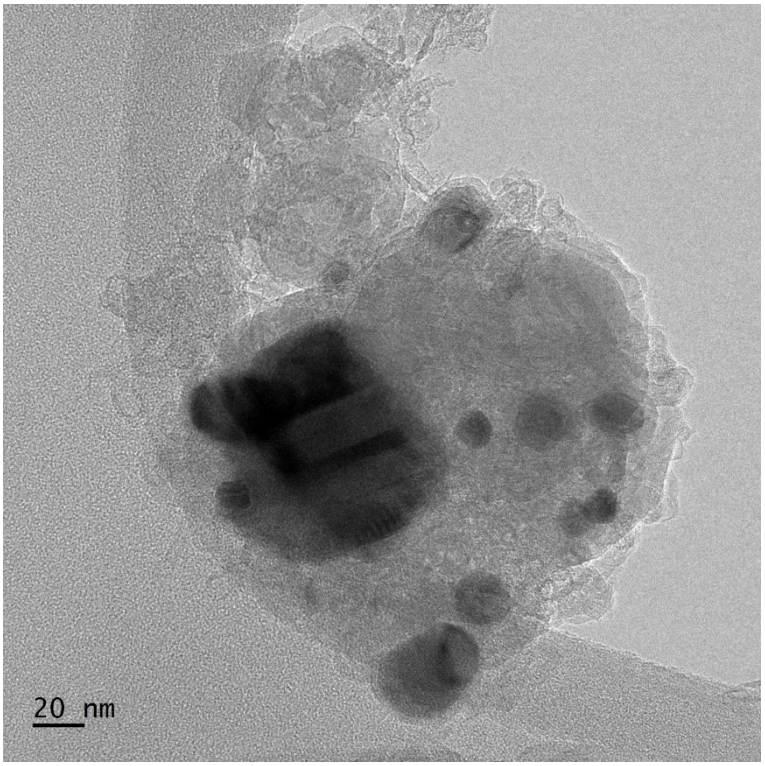

Figure S4. TEM image of c-ZIF-67

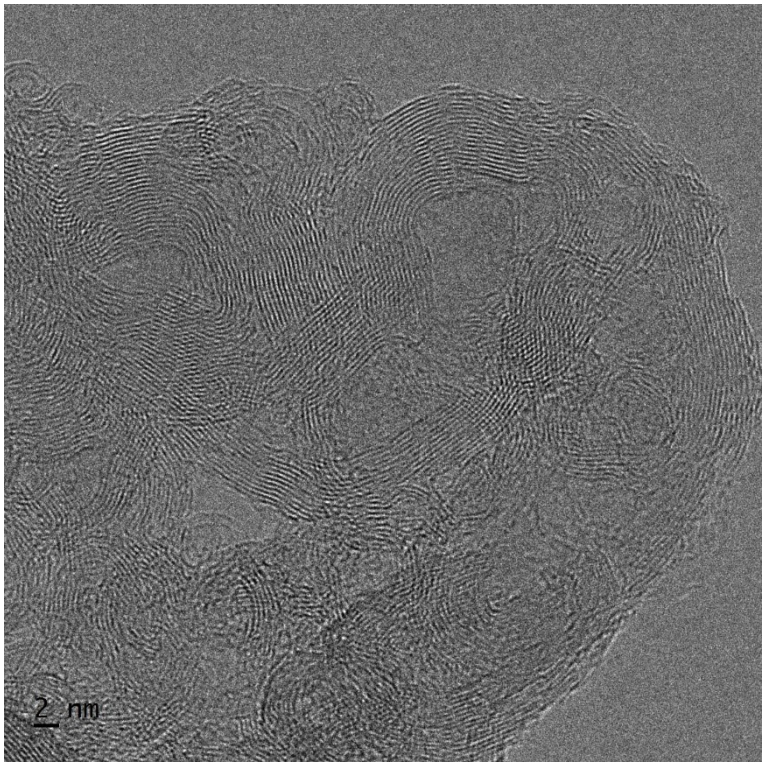

Figure S5. Zoom-in TEM image of c-ZIF-67

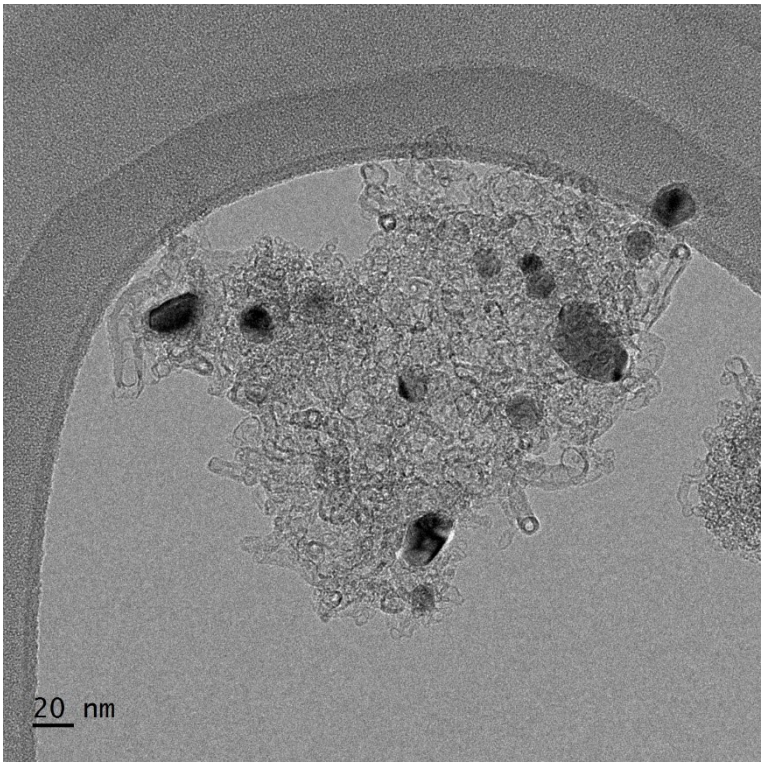

Figure S6. TEM image of c-hZIF-8

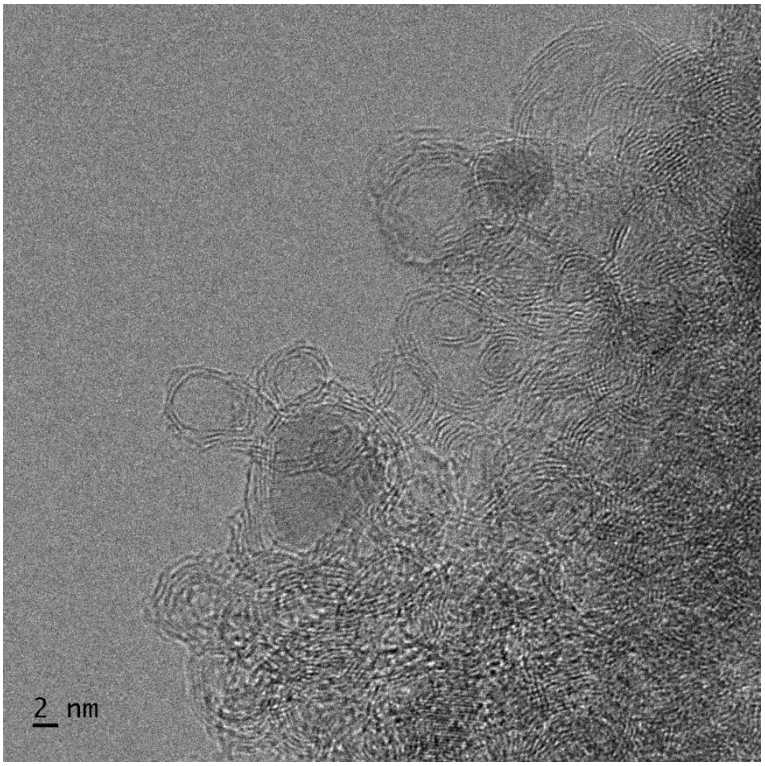

Figure S7. Zoom-in TEM image of c-hZIF-8

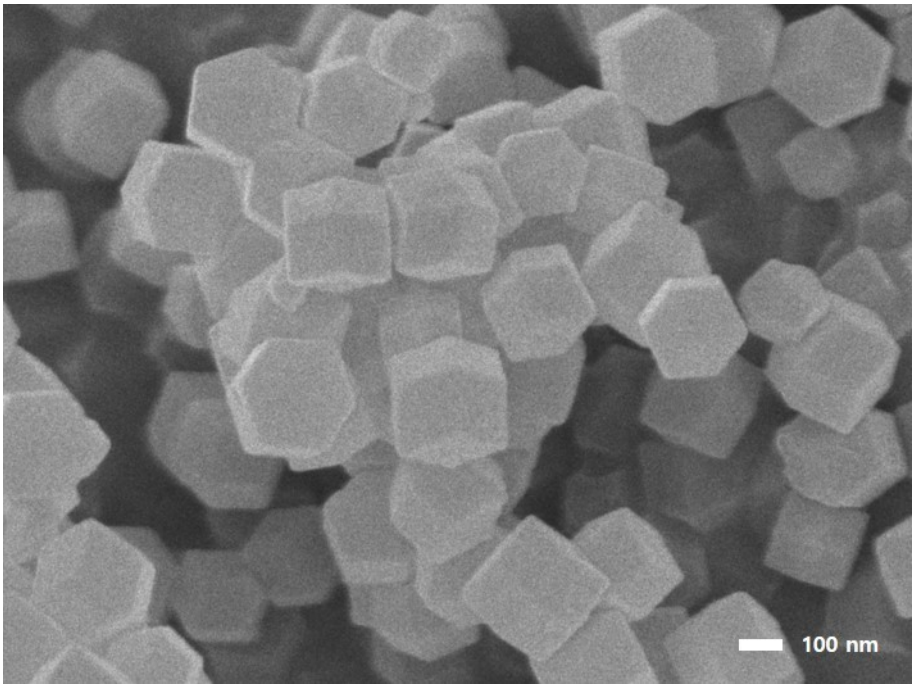

Figure S8. SEM image of ZIF-67@ZIF-8

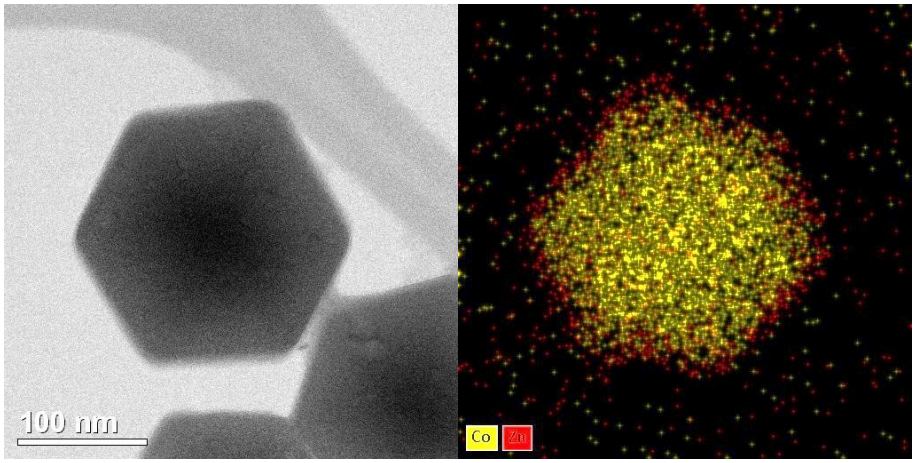

Figure S9. TEM and EDS image of ZIF-67@ZIF-8

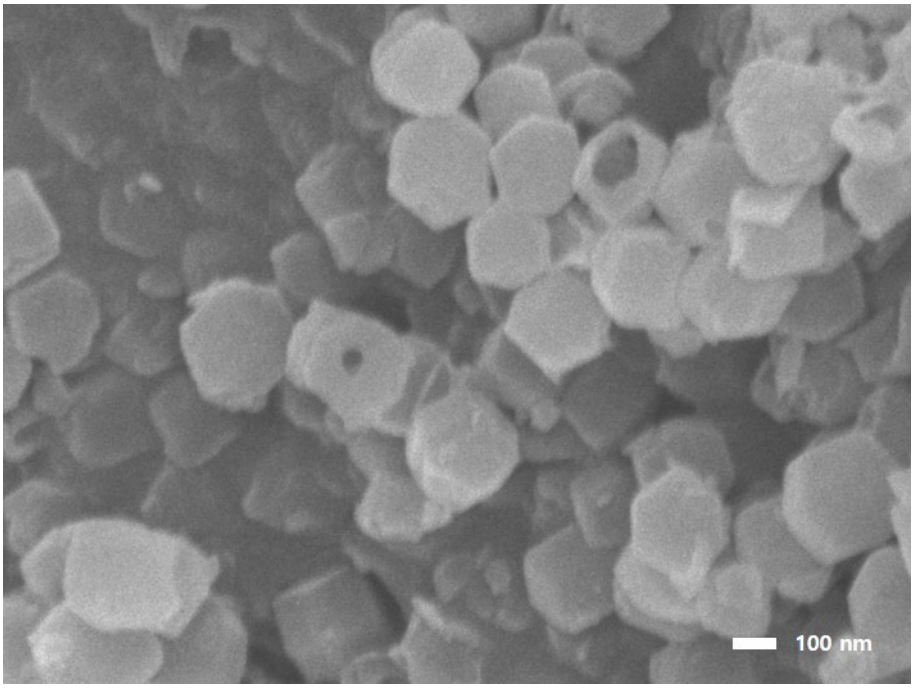

Figure S10. SEM image of hZIF-8

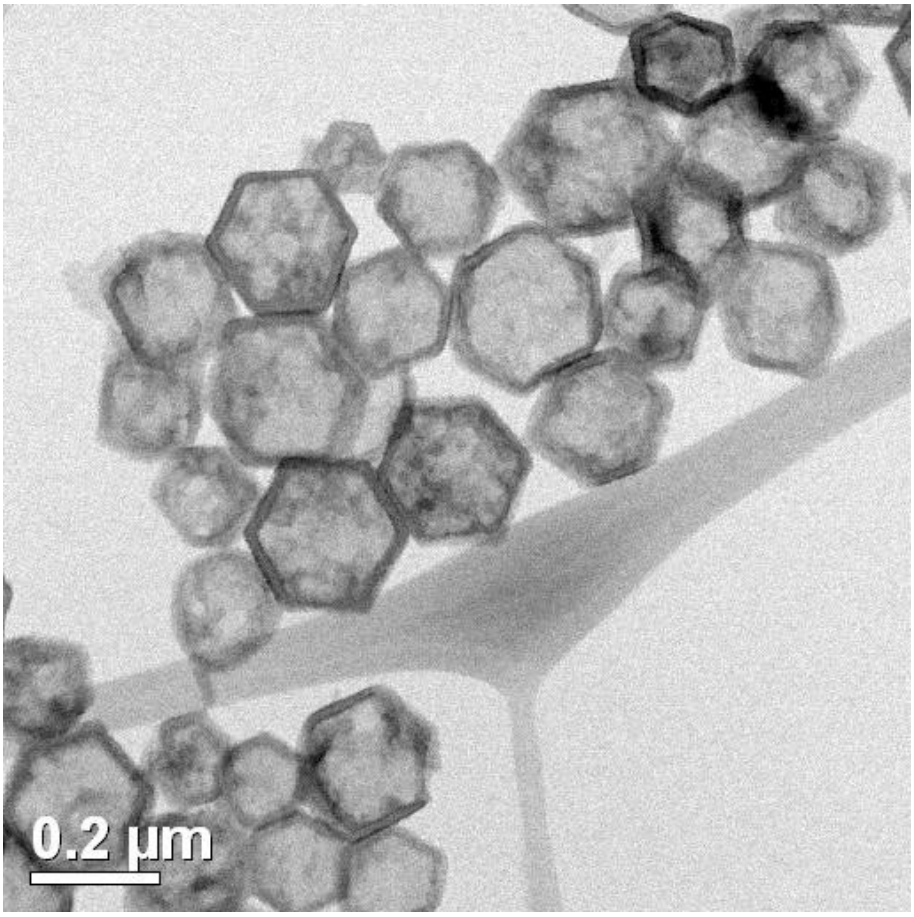

Figure S11. TEM image of hZIF-8

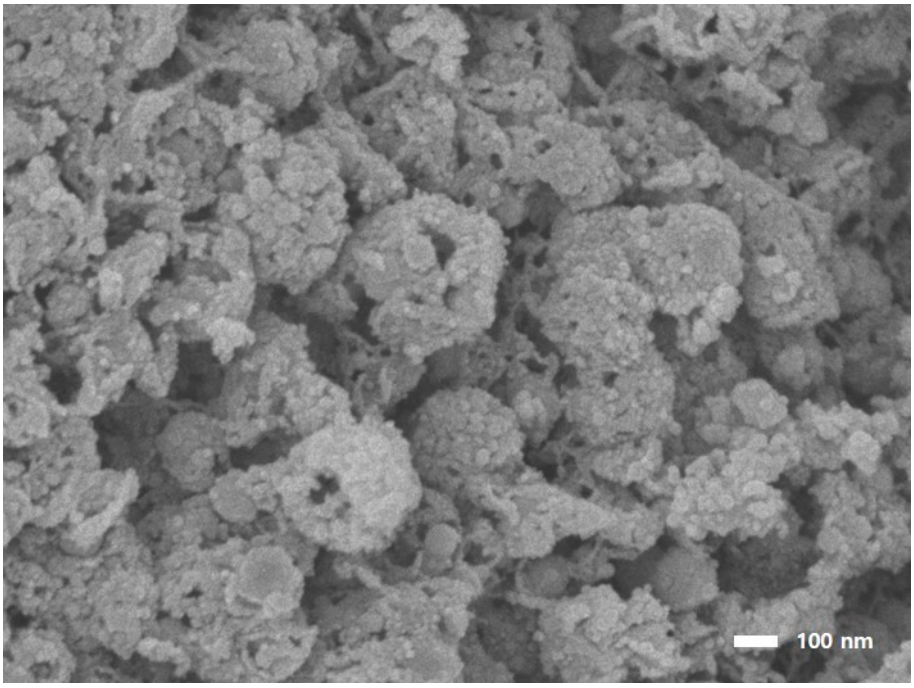

Figure S12. SEM image of c-hZIF-8

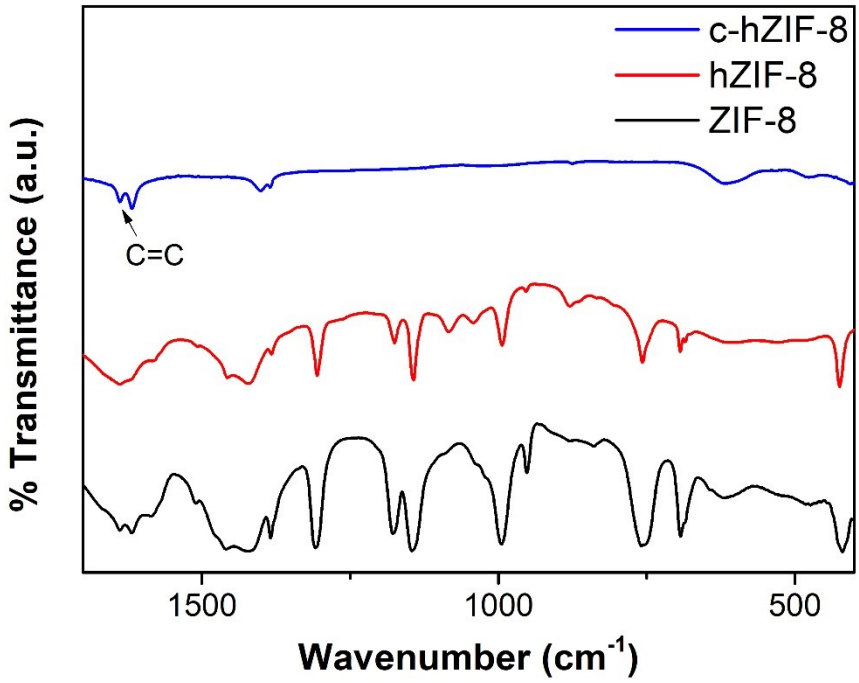

Figure S13. FT-IR spectra of ZIF-8, hZIF-8, and c-hZIF-8

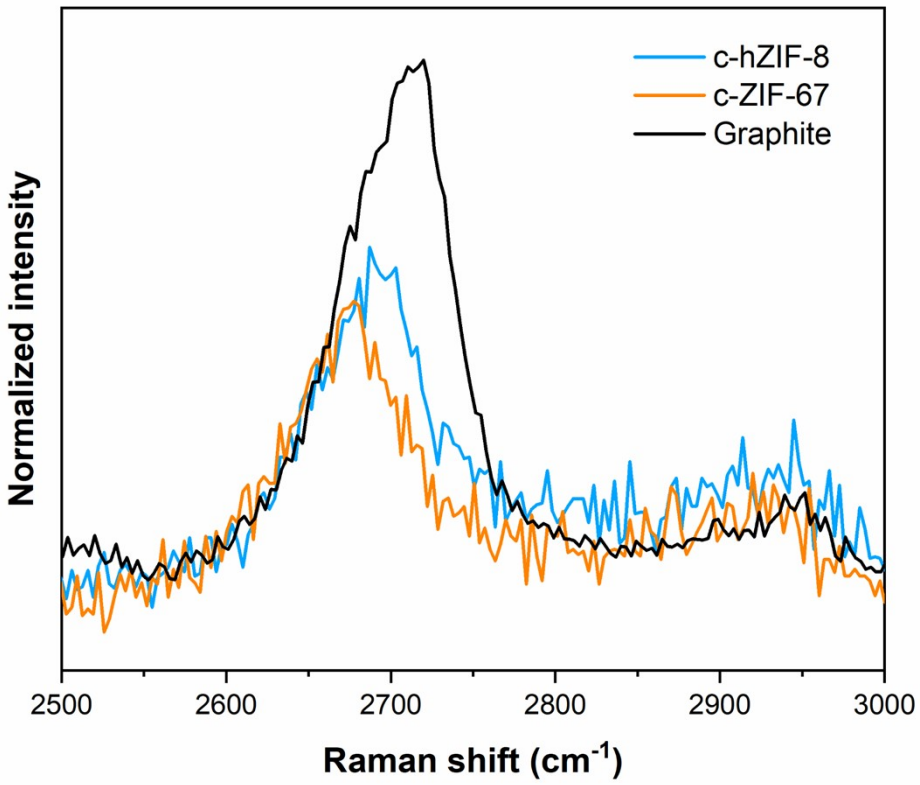

Figure S14. Raman Spectra of c-hZIF-8, c-ZIF-67, and graphite

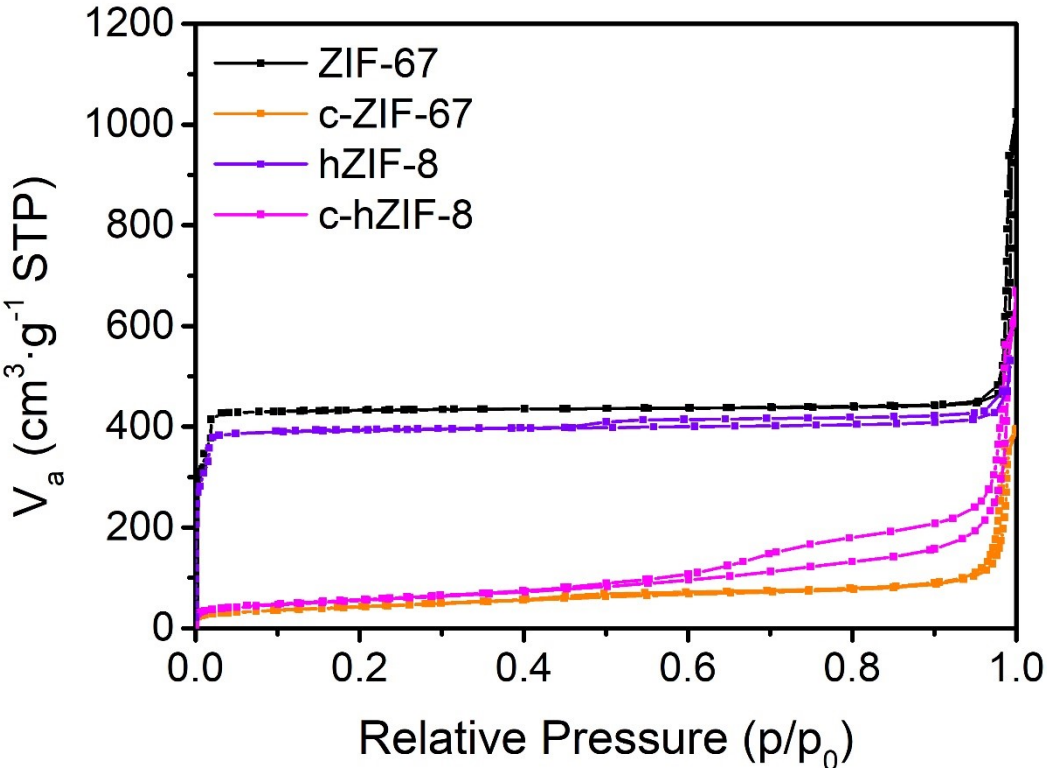

Figure S15. Nitrogen adsorption-desorption isotherms of ZIF-67, c-ZIF-67, hZIF-8, and c-hZIF-8

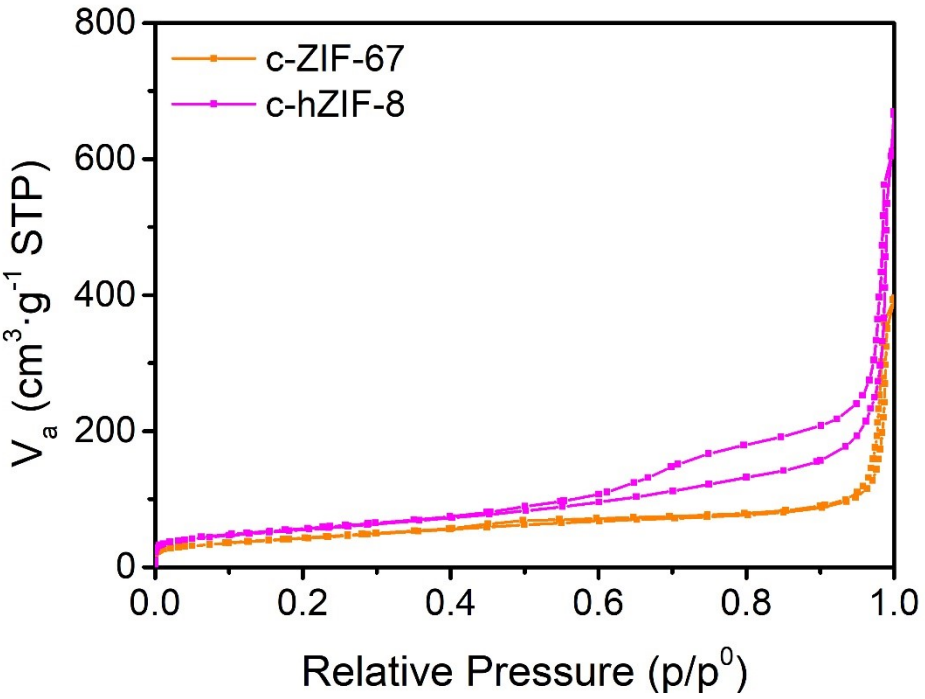

Figure S16. Nitrogen adsorption-desorption isotherms of c-ZIF-67 and c-hZIF-8

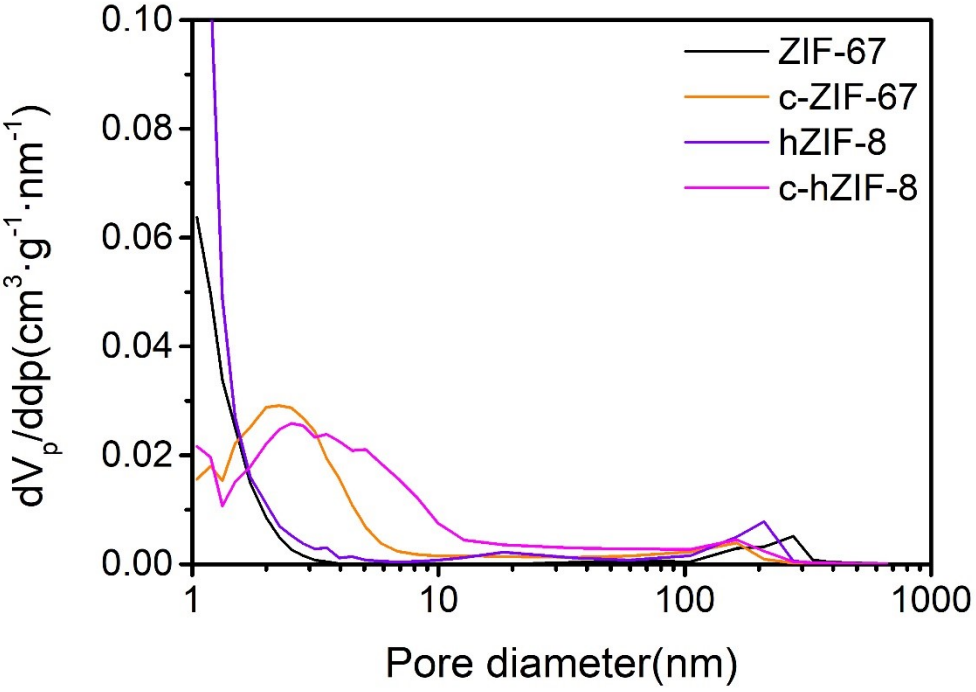

Figure S17. Pore distribution of ZIF-67, c-ZIF-67, hZIF-8, and c-hZIF-8

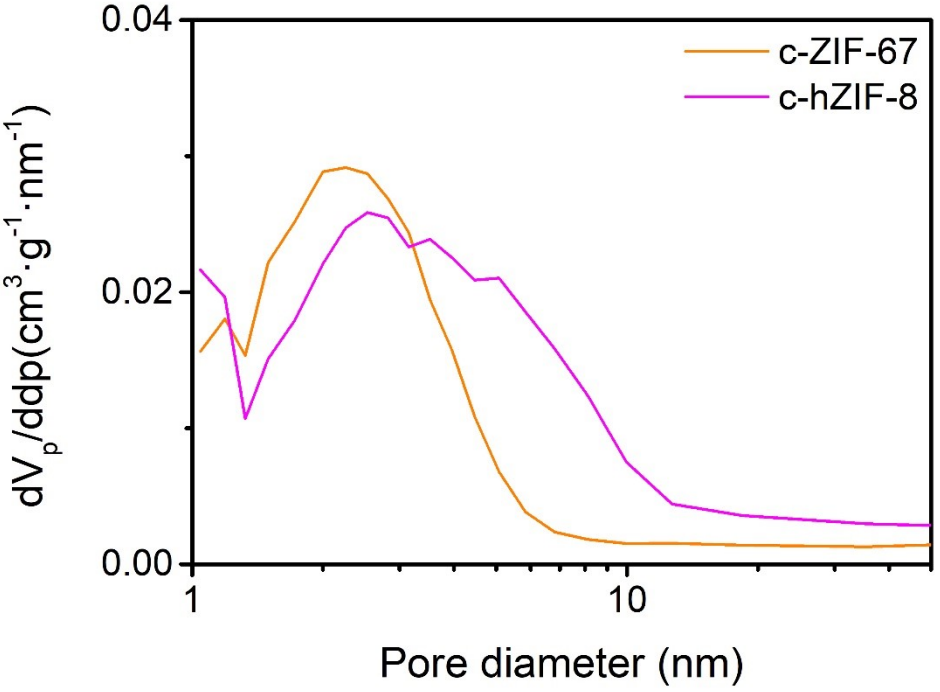

Figure S18. Pore distribution of c-ZIF-67 and c-hZIF-8

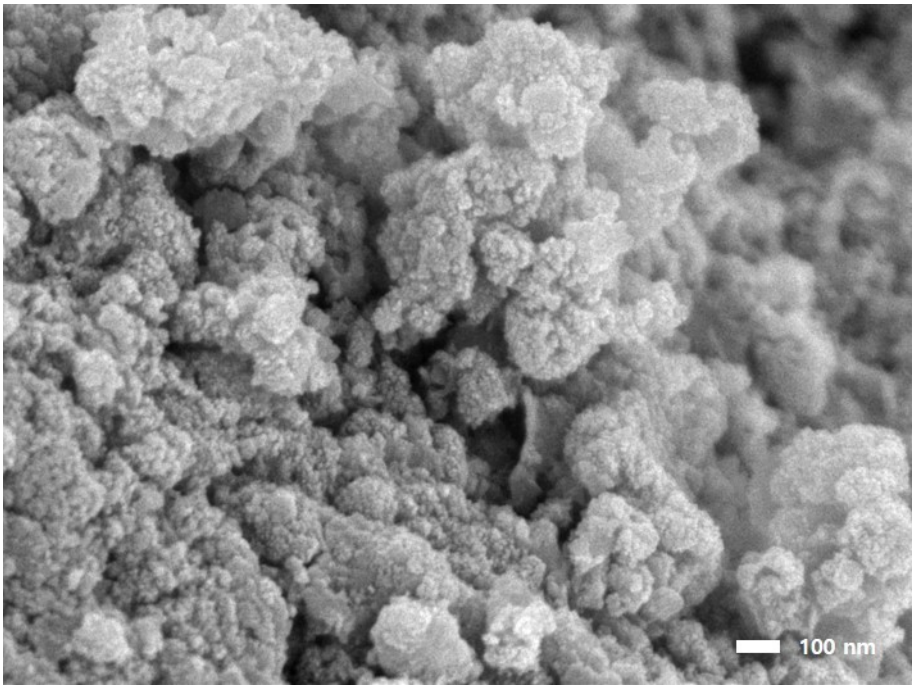

Figure S19. SEM image of $Co(OH)_2 \subset$c-hZIF-8

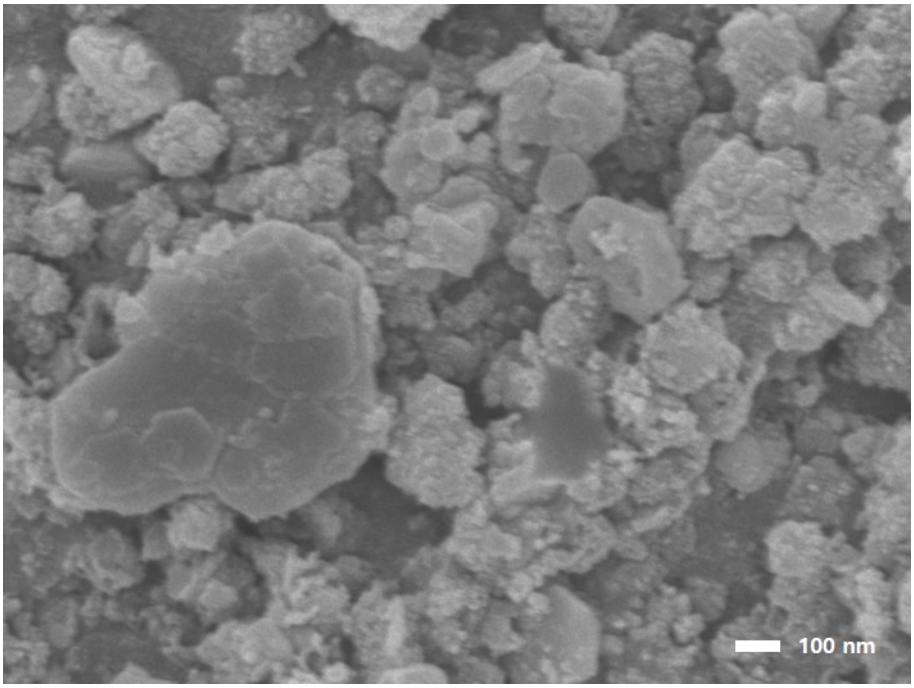

Figure S20. SEM image of $Co(OH)_2 \subset$c-ZIF-67

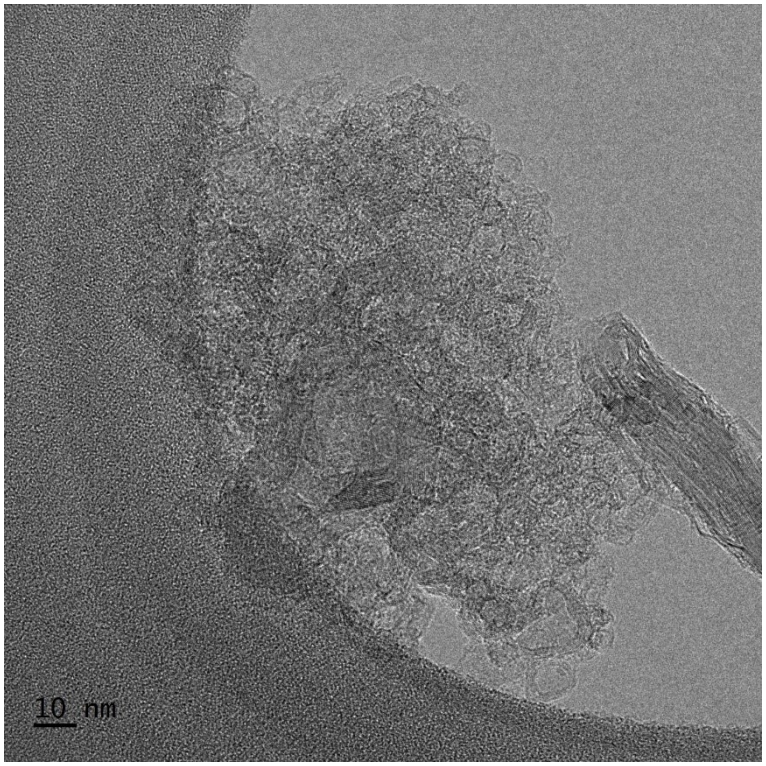

Figure S21. TEM image of $Co(OH)_2 \subset$c-hZIF-8

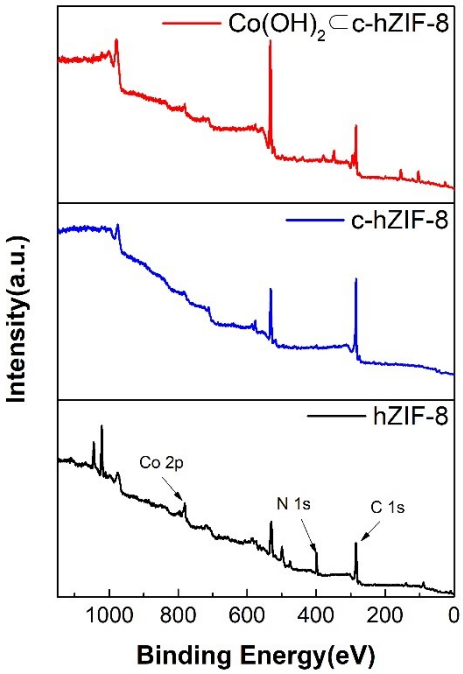

Figure S22. XPS survey of hZIF-8, c-hZIF-8, and $Co(OH)_2 \subset$c-hZIF-8

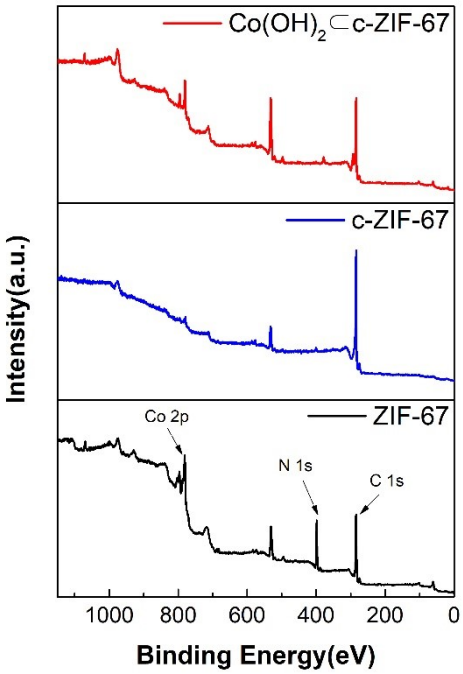

Figure S23. XPS survey of ZIF-67, c-ZIF-67, and $Co(OH)_2 \subset$c-ZIF-67

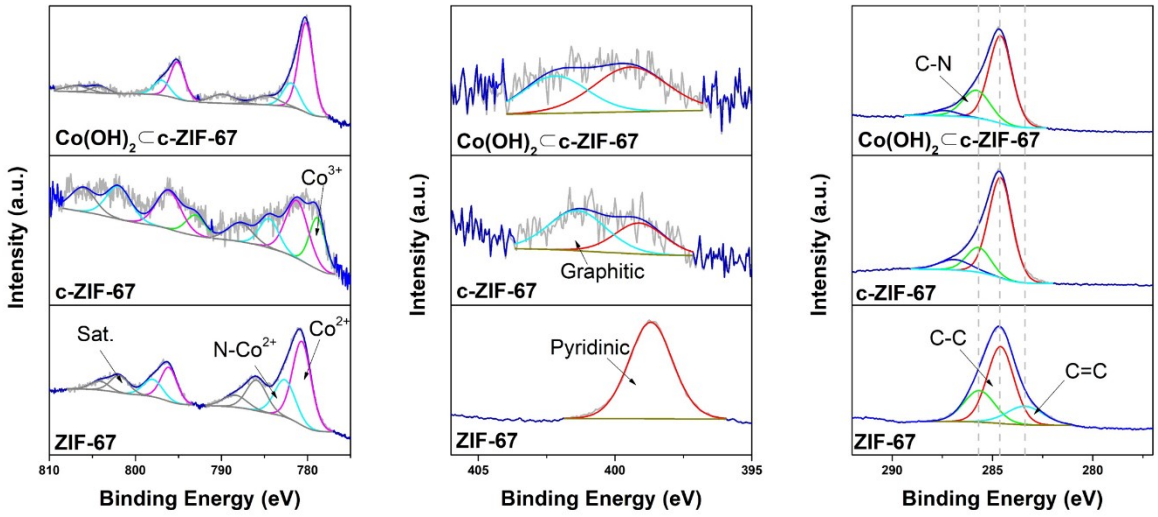

Figure S24. XPS Co 2p, N 1s, and C 1s spectra of ZIF-67, c-ZIF-67, and $Co(OH)_2$⊂c-ZIF-67

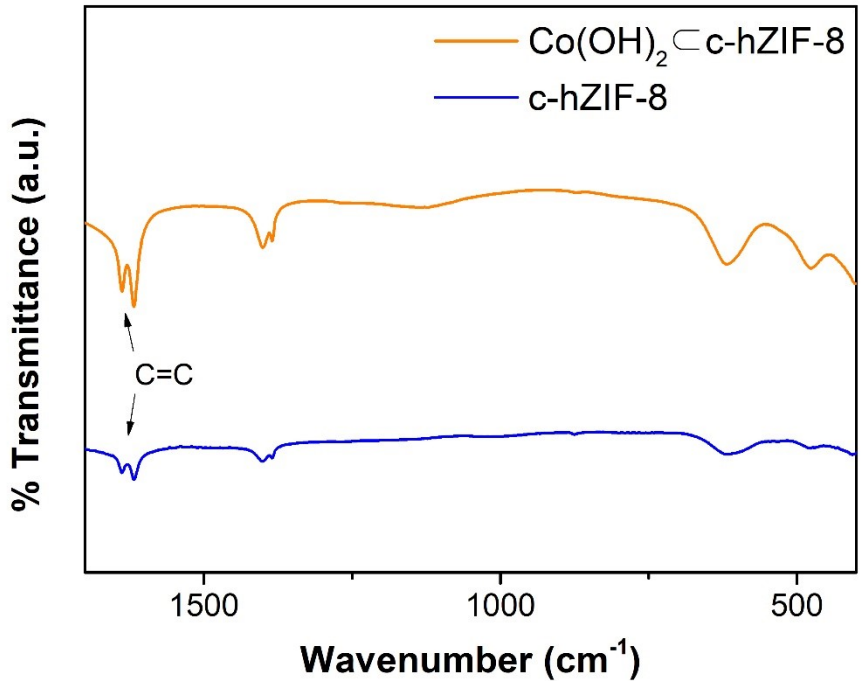

Figure S25. FT-IR spectra of c-hZIF-8 and $Co(OH)_2 \subset$c-hZIF-8

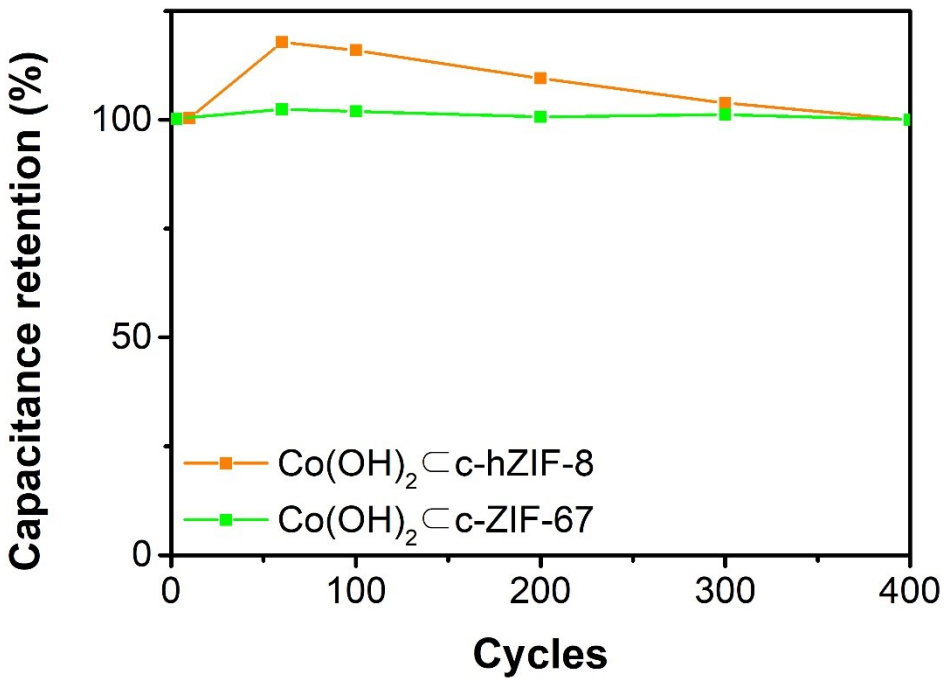

Figure S26. Capacitance Retention Rate of $Co(OH)_2 \subset$c-hZIF-8 and $Co(OH)_2 \subset$c-ZIF-67 during activation step

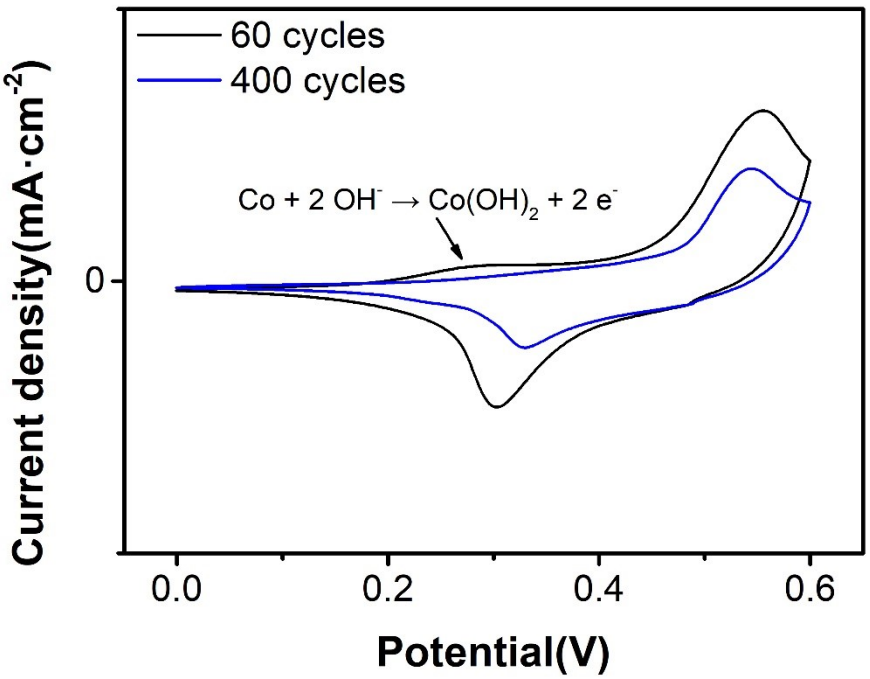

Figure S27. Cyclic voltammetry curve of $Co(OH)_2 \subset$c-hZIF-8 during the activation step

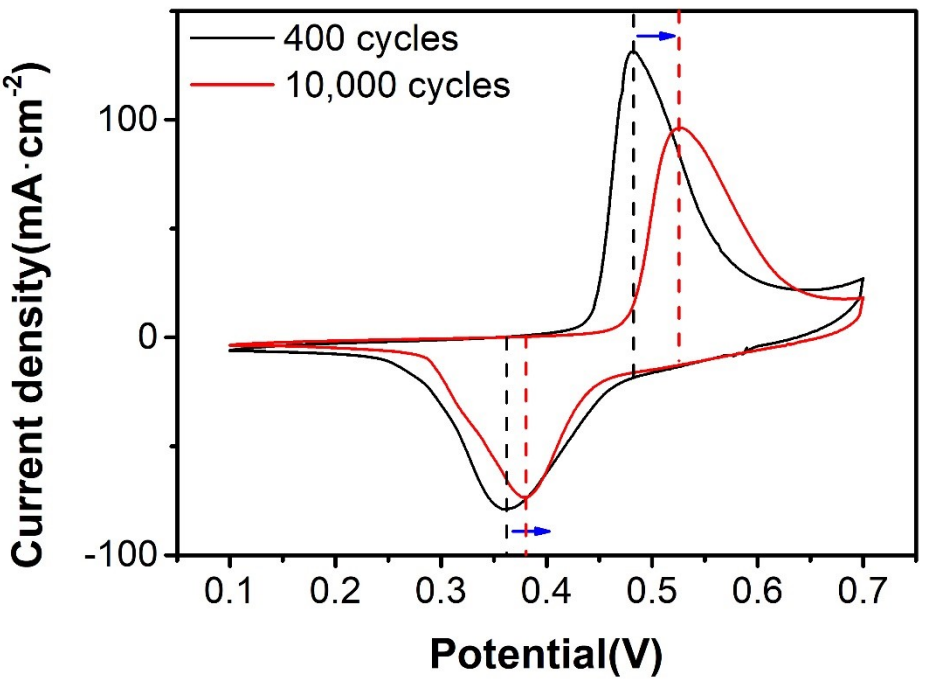

Figure S28. Cyclic voltammetry curve peak shift of $Co(OH)_2 \subset$c-hZIF-8

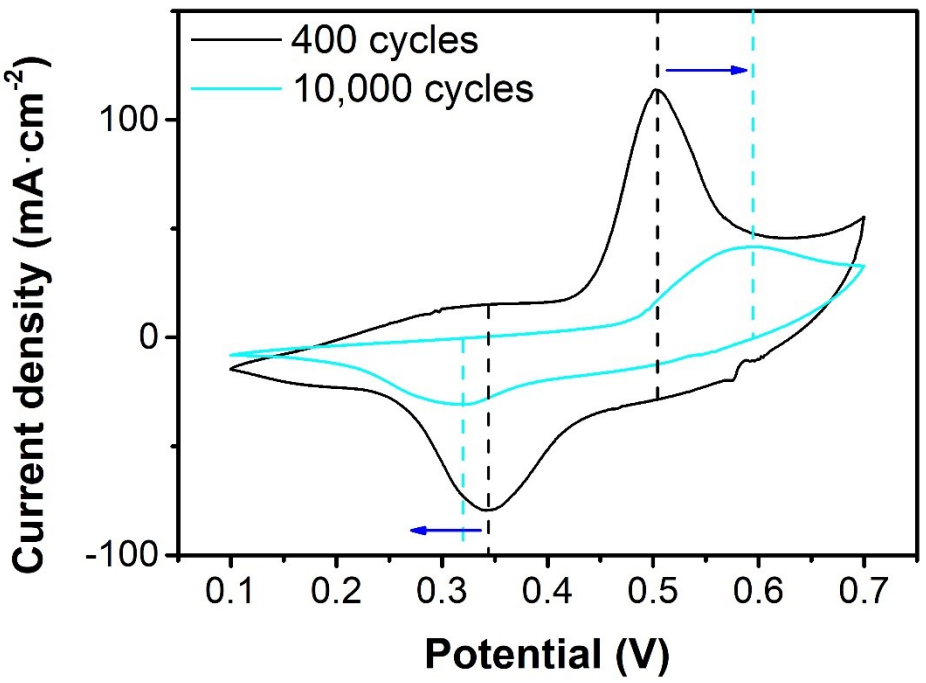

Figure S29. Cyclic voltammetry curve peak shift of $Co(OH)_2 \subset$c-ZIF-67

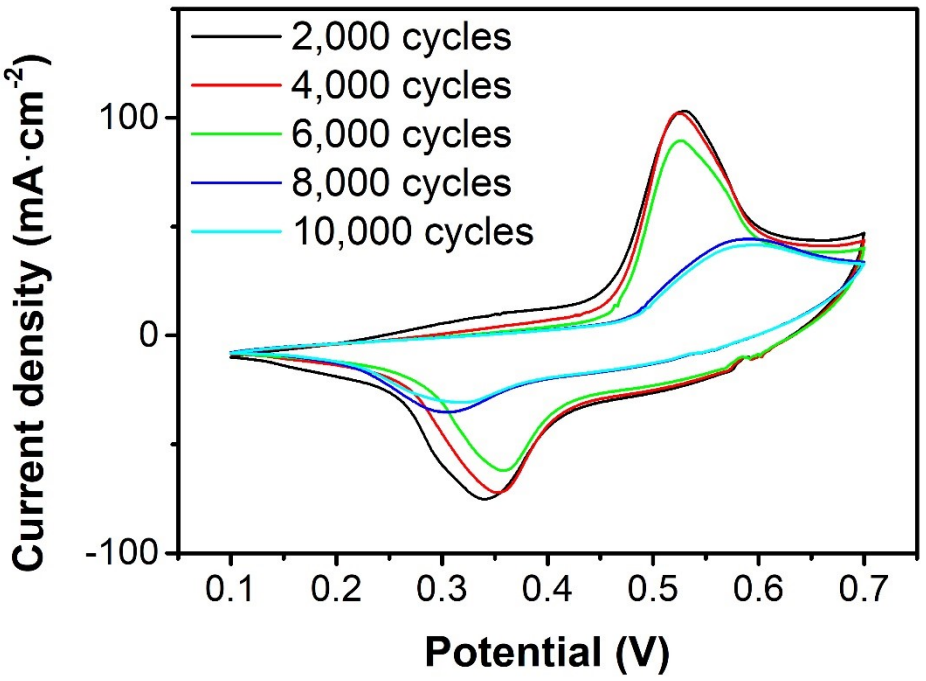

Figure S30. Cyclic voltammetry curve monitored every 2000 cycles of $Co(OH)_2$⊂c-ZIF-67

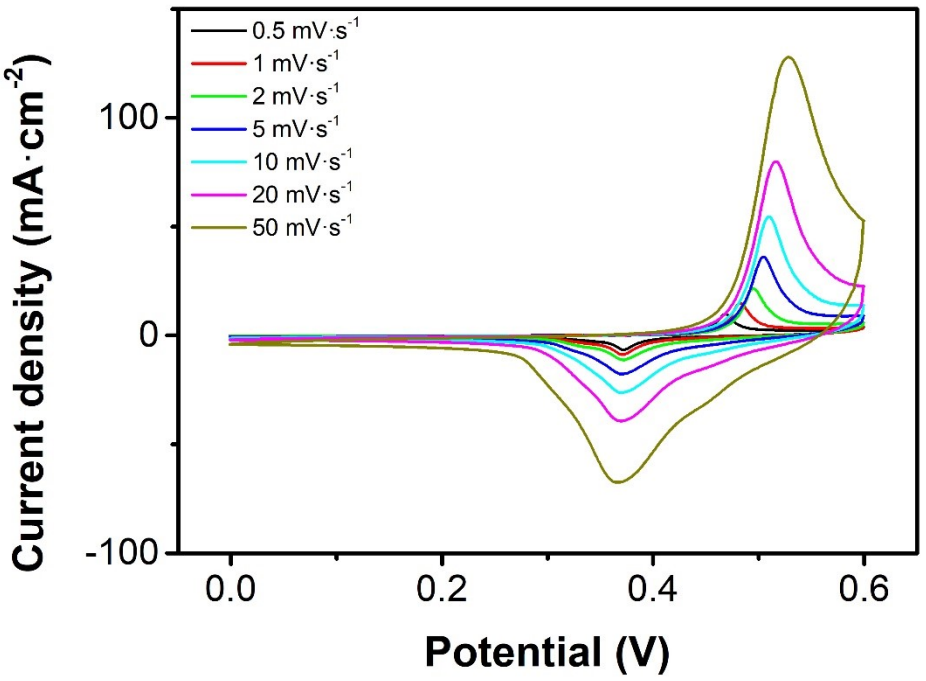

Figure S31. Cyclic voltammetry curve of $Co(OH)_2 \subset$c-hZIF-8 at 0.5 to 50 $mV \cdot s^{-1}$

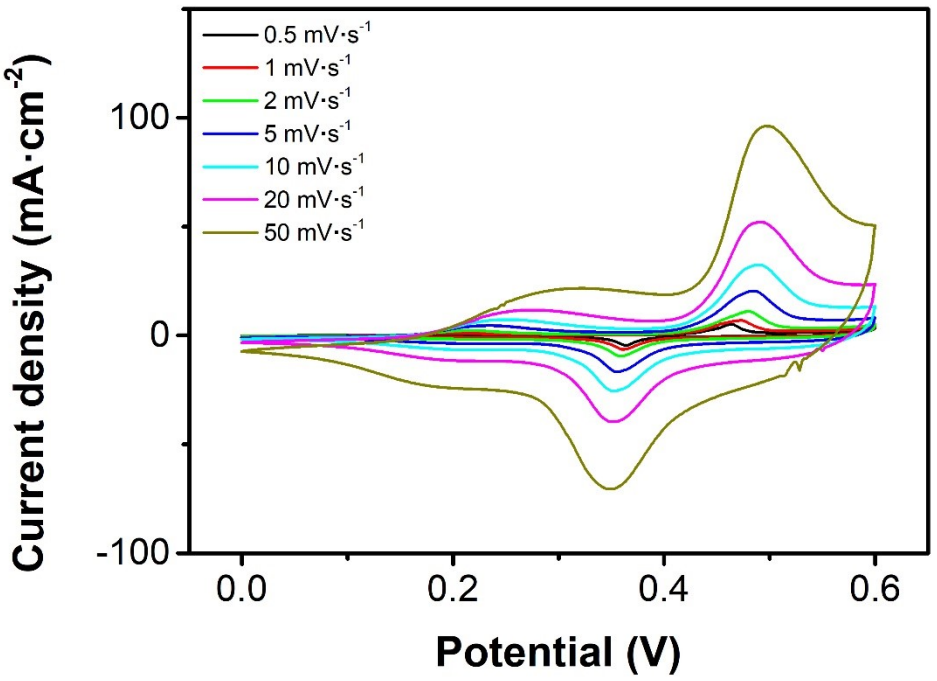

Figure S32. Cyclic voltammetry curve of $Co(OH)_2 \subset$c-ZIF-67 at 0.5 to 50 $mV \cdot s^{-1}$

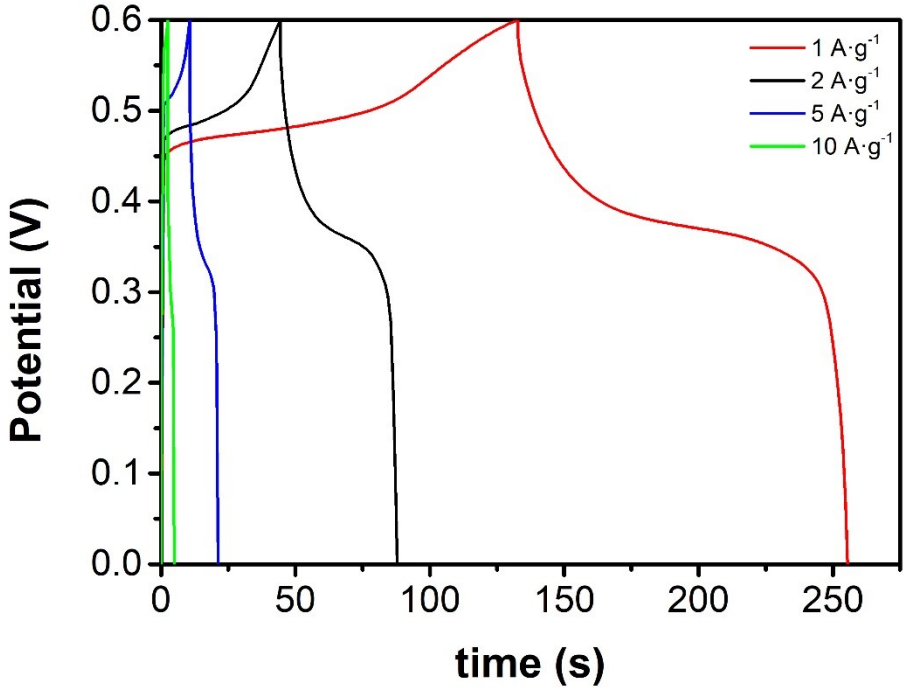

Figure S33. Galvanostatic charge-discharge curve of c-hZIF-8 at 1 to 10 A·g^{-1}

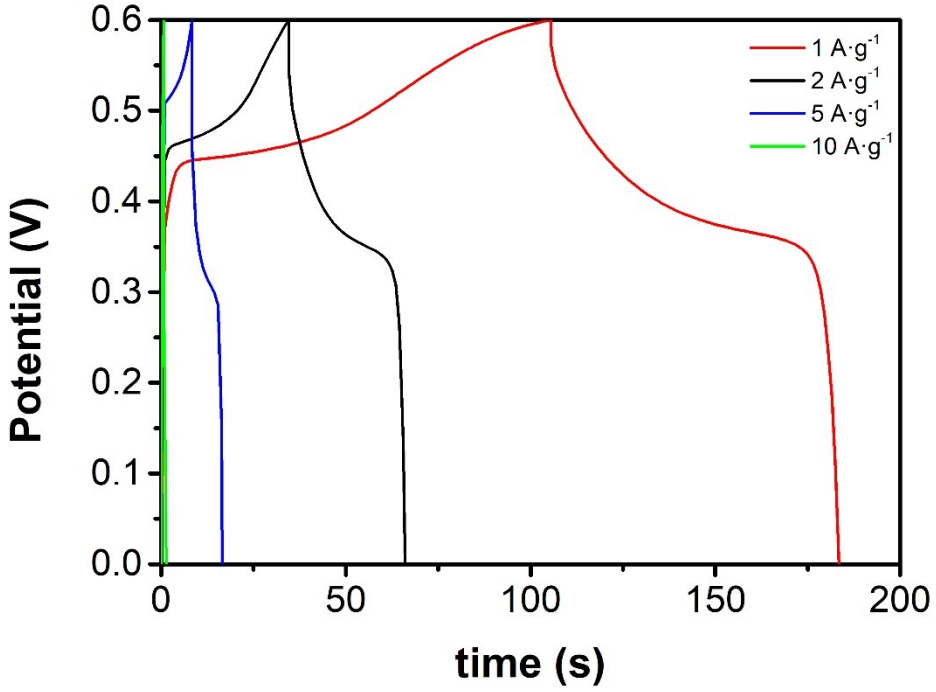

Figure S34. Galvanostatic charge-discharge curve of c-ZIF-67 at 1 to 10 A·g^{-1}

	specific surface area [$m^2 \cdot g^{-1}$]	average pore size [nm]	Total pore volume [$cm^3 \cdot g^{-1}$]
ZIF-67	1685	2	0.87
c-ZIF-67	154	14	0.53
hZIF-8	1063	4	0.72
c-hZIF-8	197	17	0.79

Table S1. BET Specific surface area, average pore diameter, and total pore volume of ZIF-67, c-ZIF-67, hZIF-8, and c-hZIF-8

Current density [A·g^{-1}]	Specific capacitance [F·g^{-1}]
1	257.2
2	176.3
5	98.9
10	76.4

.

Table S2. The specific capacitance of $Co(OH)_2$⊂c-hZIF-8 at different current densities

Current density [A·g^{-1}]	Specific capacitance [F·g^{-1}]
1	169.2
2	129.8
5	71.9
10	6.1

.

Table S3. The specific capacitance of $Co(OH)_2$⊂c-ZIF-67 at different current densities